Journal of Environmental Health and Sustainable Development

Preparation of Nanosized Zero-Valent zinc (Zn^0) Immobilized on ZnO as Redox Nanocomposite for Degradation of Methyl Orange from Aqueous Solution

Samira Taherkhani [1], Ali Khani [2*]

[1] *Department of Chemistry, Faculty of Science, University of Zanjan, Zanjan, Iran.*
[2] *Department of Chemistry and Chemical Engineering, Miyaneh Branch, Islamic Azad University, Miyaneh, Iran.*

ARTICLE INFO

ORIGINAL ARTICLE

Article History:
Received:23 October 2018
Accepted: 20 January 2019

***Corresponding Author:**
Ali Khani
Email:
a.khani59@yahoo.com
Tel:
+984152225317

Keywords:
Redox Nanocomposite,
Methyl Orange Dye,
Waste Water.

ABSTRACT

Introduction: In this study, nanosized zero-valent zinc (Zn^0) as a reducing agent, simultaneously synthesized and immobilized on an oxidizing agent, ZnO photocatalyst for degradation of methyl orange (MO) from the aqueous solution.
Materials and Methods: The prepared redox nanocomposite (nZn^0-ZnO) was characterized by the XRD and SEM techniques. The prepared sample was separated by centrifuging. The preparation process of nZn^0-ZnO including synthesis-immobilization, washing, and drying carried out under Argon gas flow. Moreover, the effect of temperature and kinetics reaction was studied.
Results: The results showed that degradation efficiency of prepared redox nanocomposite was increased compared to each ZnO nanopowder and Zn^0 under the same operational condition. The calculated activation energy for the degradation process was 4.05 $KJ.mol^{-1}$. Finally, the results showed that the degradation processes followed pseudo first order kinetic model in the basic condition by the relative deviation modulus.
Conclusion: As compared to ZnO nanopowder and Zn^0, the prepared redox nanocomposite showed high degradation efficiency for the removal of methyl orange from the aqueous solution.

Citation: Taherkhani S, Khani A. **Preparation of Nanosized Zero-Valent zinc (Zn^0) Immobilized on ZnO as Redox Nanocomposite for Degradation of Methyl Orange from Aqueous Solution**. J Environ Health Sustain Dev. 2019; 4(1): 694-700.

Introduction

Azo dyes pollutants are being increased in the environment because of wide uses in various industries such as textile, paper and some other related industries. Their toxic and low biodegradation rate has obligated the researchers to focus on an efficient and low-cost method for treatment of azo dyes [1].

Various processes have been proposed for wastewater treatment including adsorption [2, 3], floatation and sedimentation [4], coagulation-flocculation [5], biological treatment [6], reduction with zero-valent metals [7] and advanced oxidation processes (AOPs) such as UV/H_2O_2, UV/O_3, UV/Fenton's reagent, etc [8]. Photocatalysis process with semiconductor is one of AOPs that is used for photodegradation of various organic pollutants [9] and also, utilization of zero-valent metals such as Fe^0 (ZVI) as a reducing agent, has received wide attention [10]. In the previous studies, the removal of several pollutants such as chlorinated organics [11, 12], azo dyes [13], chlorinated organic compounds [14, 15] and metals [16, 17] has been reported by the reduction process.

[Downloaded from jehsd.ssu.ac.ir on 2025-09-12]
[DOR: 20.1001.1.24766267.2019.4.1.5.3]
[DOI: 10.18502/jehsd.v4i1.486]

However, these approaches are not without their disadvantages, particularly the inability to complete mineralization (depredating to inorganic materials) [18]. For this reason, the researchers focused on integrated processes for complete mineralization of pollutants, especially azo dyes.

Chang et al. reported an integrated technique including zero-valent iron and UV/H_2O_2 processes for complete mineralization of an azo dye [19]. In another research, Shu et al. integrated nanosized zero-valent iron (NZVI) particles with UV/H_2O_2 process for more decolorization of acid black 24 [20]. They reported that the reduction process by NZVI was connected to the UV/H_2O_2 process; so, it could solve the above problem and thoroughly eliminated TOC up to complete color reduction when 93.9% TOC removal was achieved. Also, Khani et al. used nanosized zero-valent iron-ZnO photocatalyst system for more degradation of acid orange [7].

Thus, in full mineralization, integrating (connecting) the two processes such as the zero-valent metal reduction and photooxidation were proposed to obtain complete decolorization and mineralization. It also saved time and energy [7].

In this study, the prepared redox nanocomposite (nano zero-valent zinc immobilized on nano zinc oxide) employs both of reductive decolorization and photodegradation processes for the removal of methyl orange (MO) with zero-valent zinc (Zn^0) and ZnO photocatalyst, respectively.

Materials and Methods

Chemicals and materials

Methyl orange as a pollutant was supplied from Boyakhsaz Co. (Iran). $NaBH_4$, $ZnCl_2$ and nanosized zinc oxide (45 nm) were obtained from Merck (Germany). Deionized water was used in all experiments.

Preparation of redox nanocomposite (nZn^0-ZnO)

The nanosized zero-valent zinc (Zn^0) particles were chemically synthesized. That way, 250 ml of $ZnCl_2$ solution (1000 $mg.L^{-1}$) was stirred with 5g nanoparticles of ZnO in deionized water (dispersed by ultrasonication) for one hour until aqueous zinc chloride (Zn^{2+}) was adsorbed to ZnO [20]. The borohydride solution (2000 $mg.L^{-1}$ and approximately 100ml) was then added dropwise to the aqueous zinc chloride and ZnO mixture at room temperature while stirring thoroughly using a magnetic mixer. The gray solid particles of nZVZ appeared immediately following the addition of a few drops of $NaBH_4$ solution. After the full addition of the borohydride solution, the mixture was thoroughly stirred for a further 30 minutes. The reduction of zinc with borohydride ions can be represented according to the following equation:

$$3Zn^{2+} + 6BH_4^- + 18H_2O \longrightarrow 3Zn^0 + 6B(OH)_3 + 21H_2 \quad (1)$$

The prepared sample was separated by centrifuging. The preparation process of nZn^0-ZnO including synthesis-immobilization, washing, and drying carried out under Argon gas flow. To evaluate supporting treatment, nZn^0-ZnO was leached twice with deionized water and then dried (in the oven for one hour under Argon gas flow). During the treatment, tangible weight difference of prepared sample (nanocomposite) was not observed which indicates ZVZ immobilized on ZnO, properly.

A Leo 440i scanning electron microscope (SEM) followed by Au coated by the sputtering method using a coater sputter SC 761 were applied to determine the morphology of the prepared redox nanocomposite.

Redox degradation experiment

For the redox degradation of MO, a solution was prepared that contained the known concentrations of MO. Then, one liter of the prepared solution was transferred into the designed photoreactor (Figure 1) and agitated with a magnetic stirrer during the experiment. To evaluate the effect of temperature on redox degradation, the solution temperature was adjusted with a heating-cooling system. Then the UV-C lamp (8 W, Philips, the light intensity of 0.4 klx measured with a lux meter, Leybold-Heraeus) was switched on, and the experiment began. The concentration of the MO solution was determined with total organic carbon (TOC) analyzer (Shimadzu TOC-VCSH, North America). The removal degree of MO was calculated at different time (0-90 min) intervals using the

[Downloaded from jehsd.ssu.ac.ir on 2025-09-12]
[DOR: 20.1001.1.24766267.2019.4.1.5.3]
[DOI: 10.18502/jehsd.v4i1.486]

equation given below:

$$X\,\% = \frac{C_0 - C_t}{C_0} \times 100 \qquad (2)$$

X% is the percent removal, C_0 is the initial concentration of MO, and C_t is the concentration of MO at the time, t. All experiments were done three times (variance = 0.044), and the experiments were performed in the designed batch reactor (Figure 1).

Kinetics study experiment

For a kinetics study in different temperatures and for determining the activation energy (E_a) of redox degradation reaction, the effect of temperature on the degradation process was first evaluated. For this purpose, the experiments were carried out at different temperatures varying from 278.15 to 318.15 K and other parameters such as C_0, T, pH, etc., were kept under basic conditions (C_0 of MO = 50 $mg.L^{-1}$, the mass of nanocomposite = 5g, pH = 7, T = 25 ºC, the volume of solution = 1 L, and reaction time = 90 min).

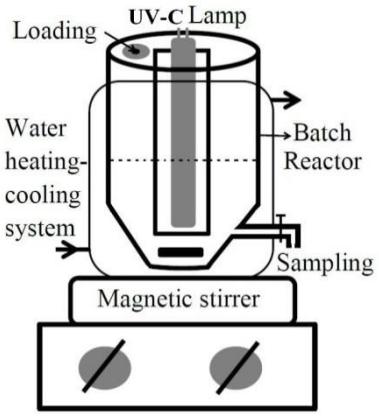

Figure 1: The schematic diagram of experimental apparatus which is consisted of jacketed cylindrical with conical bottom Pyrex (D = 5 cm and length = 20 cm) for degradation of MO.

Results

Redox nanocomposite characterization

The results from X-ray Diffraction (XRD) analysis are shown in Figure 2. The average crystallite size (D in nm) of Zn^0 nanoparticles was determined using XRD (Bruker) pattern of the redox nanocomposite according to the Scherrer equation [8]:

$$D = k\frac{\lambda}{\beta.Cos\ \theta} \qquad (3)$$

K is a constant which is 0.89, λ is the XRD wavelength which is 0.154 nm, β is the full width at half maximum (0.0036 Radian), and θ is the half diffraction angle which is 21 (2Θ = 42).

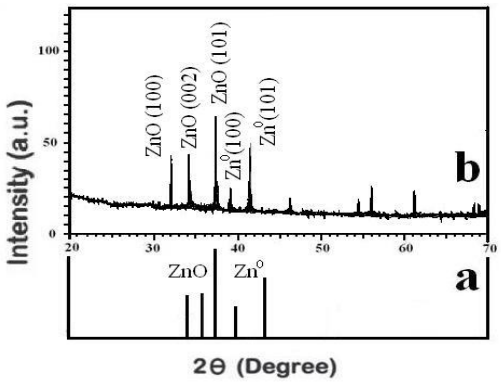

Figure 2: Standard Zn-ZnO powder diffraction pattern (a) and XRD pattern of nano nZ^0-ZnO

[Downloaded from jehsd.ssu.ac.ir on 2025-09-12]
[DOR: 20.1001.1.24766267.2019.4.1.5.3]
[DOI: 10.18502/jehsd.v4i1.486]

The calculation indicates that the average particle size of Zn^0 is about 100 nm. Besides, this figure clearly shows the same pattern for the prepared nZn^0-ZnO comparing to the standard Zn-ZnO powder.

Figure 3 shows the SEM image of the surface of the prepared nanocomposite. The SEM analysis demonstrated that the most particles of prepared nanocomposite have particle sizes below 100 nm.

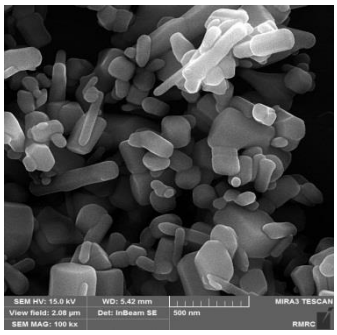

Figure 3: The SEM image of nZ^0-ZnO.

Comparative study

To evaluate the efficiency of prepared redox nanocomposite in comparison with only ZnO and Zn^0, three experiments in basic conditions were designed as following: 1) reduction with nano zero-valent zinc (nZVZ), 2) photooxidation with nano ZnO /UV (nZnO/UV), and 3) reduction-oxidation with redox nanocomposite (nZVZ-ZnO) under UV-C light which is shown in Figure 4.

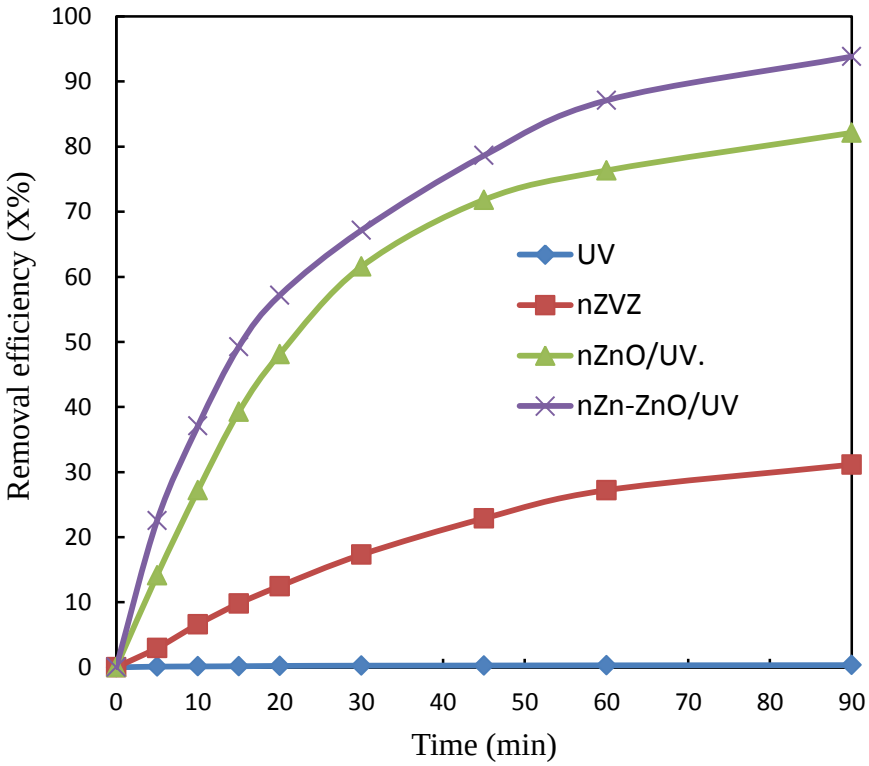

Figure 4: Removal efficiency (X%) of MO by the prepared redox nanocomposite in comparison with each of ZnO and Zn^0.

[Downloaded from jehsd.ssu.ac.ir on 2025-09-12]
[DOR: 20.1001.1.24766267.2019.4.1.5.3]
[DOI: 10.18502/jehsd.v4i1.486]

Discussion

Evaluation of the prepared redox nanocomposite efficiency

As can be seen in Figure 4, UV-C only cannot remove MO by photolysis process, and the redox nanocomposite showed the highest degradation efficiency (X% = 93.82). The degree of degradation for nZnO and nZVZ was 82.11% and 31.14% after 90 min, respectively. Figure 4 also showed that both the light (UV) and the prepared nanocomposite were needed for the effective destruction of MO [8]. Also, nZn^0-ZnO (in the darkness condition) and only UV light do not affect the adsorption and photolysis of MO.

Kinetics study

Kinetics of the redox degradation reaction was studied for calculation of the apparent rate constant (k_{app}) [8]. In the literature, the following pseudo-first-order reaction model can be used to describe the rate phenomena observed for the degradation process with solid phase nanocomposite.

$$r_{MO} = \frac{-dC_{MO}}{dt} = \frac{k_r K C_{MO}}{1 + K C_{MO}} \quad (4)$$

Where, r_{MO} is the rate of reaction (redox degradation of the solute MO), C_{MO} is the MO concentration, t is the time of the reaction, k_r and K are the reaction and adsorption constants associated with the MO, respectively.

However, in the case that the concentration is low, the term KC_{MO} is often negligible. So, the apparent reaction rate will follow a pseudo-first-order model. The equation was integrated under this assumption with boundary conditions of $C_{MO} = C_{MO,0}$ at t = 0 and yielded:

$$-\ln\left(\frac{C_{MO}}{C_{MO,0}}\right) = k_{app}\, t \quad (5)$$

$C_{MO,0}$ is the initial MO concentration, and k_{app} is the apparent first order rate constant. The catalytic reactions in many cases show this behavior [8]. The relative deviation modulus, P was used for determination of linear trend of the line (-ln ($C_{MO}/C_{MO,0}$) vs. t) (Figure 5).

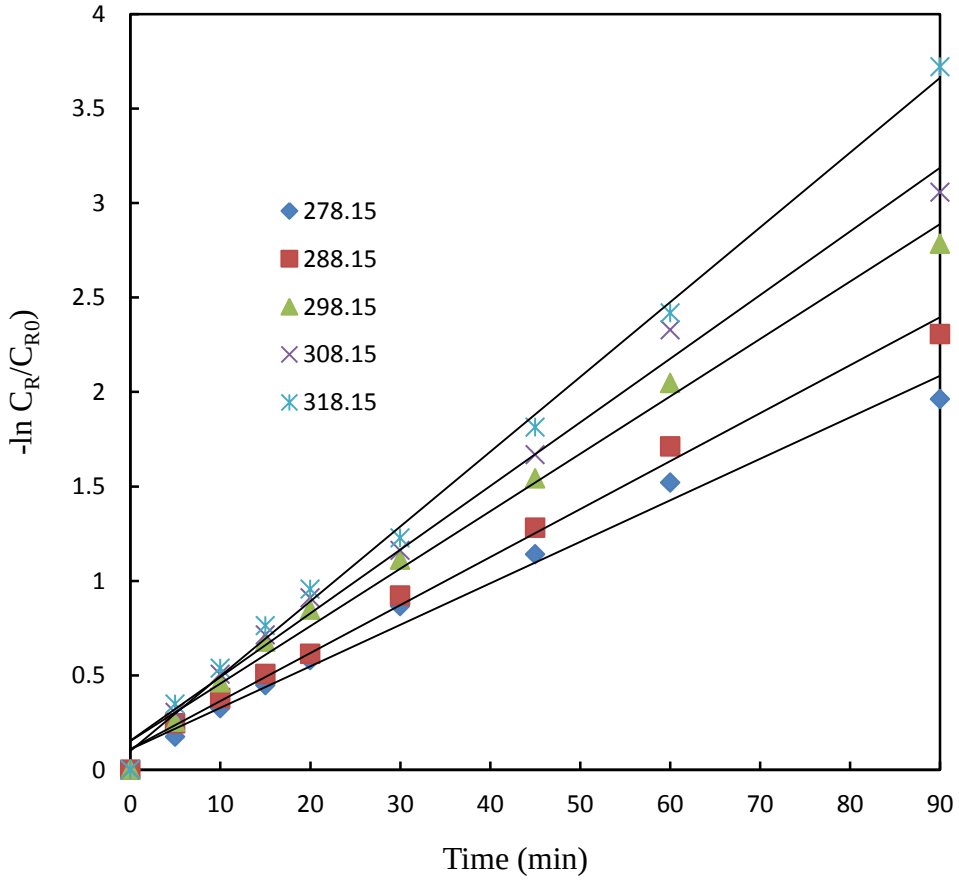

Figure 5: The plots of -ln (C_R/C_{R0}) vs. time.

[Downloaded from jehsd.ssu.ac.ir on 2025-09-12]

[DOR: 20.1001.1.24766267.2019.4.1.5.3]
[DOI: 10.18502/jehsd.v4i1.486]

When the value of P is below five, it indicates that the experimental data has suitable fitting with the straight line [2]. According to the value of P, the redox reaction follows pseudo-first-order kinetics. The apparent rate constant calculated from the slopes of the lines (-ln (C_R/C_{R0}) vs. t) is shown in Table 1.

Table 1: The apparent rate constant of reaction (k_{app}) and removal degree (X%) in different temperatures.

T (K)	278.15	288.15	298.15	308.15	318.15
X%	85.96	90.04	93.82	93.30	97.58
R^2	0.98	0.99	0.99	0.99	0.99
P	3. 35	3.02	3.85	4.01	2.92
k_{app} (min^{-1})	0.02	0.025	0.03	0.034	0.04

As shown in Table 1, the apparent rate constant (k_{app}) rises when the temperature increases. The results also indicate that the temperature increase has a significant positive effect on the reaction rate and consequently on the removal degree of MO.

Also, for the calculation of activation energy, the Arrhenius equation was used as [8]:

$$-\ln k_{app} = -\ln A + \frac{E_a}{R}\left(\frac{1}{T}\right) \quad (6)$$

k_{app}= apparent first-order rate constant in min^{-1} and T = temperature in K.

The low activation energy (E_a) value (4.05 $KJ.mol^{-1}$) suggests that redox degradation of MO is limited by diffusion step and apparent rate constant reflects the rate at which MO molecules migrate from the bulk solution to the reaction zone on the redox nanocomposite surface [9].

Conclusion

XRD analysis revealed that the crystallite size (mean coherence length) of zero-valent zinc was 28 nm. As compared to ZnO nanopowder and Zn^0, the prepared redox nanocomposite showed high degradation efficiency for the removal of methyl orange from the aqueous solution. After 90 minutes, TOC analysis showed that the removal degree (X%) of MO for nZn^0-ZnO, nano ZnO and nano Zn^0 was 93.82, 82.11 and 31.14%, respectively. The kinetics analysis demonstrated that the degradation process of MO fits well into the pseudo-first-order kinetic model on the basis of P.

Acknowledgments

The author would like to thank, Islamic Azad University (Miyaneh branch) for its financial support.

Funding

This study was funded by the Miyaneh branch, Islamic Azad University.

Conflict of interest

The authors declare that there is no conflict of interest.

This is an Open Access article distributed in accordance with the terms of the Creative Commons Attribution (CC BY 4.0) license, which permits others to distribute, remix, adapt and build upon this work for commercial use.

References

1. Fu W, Yang H, Chang L, et al. Anatase TiO_2 nanolayer coating on strontium ferrite nanoparticles for magnetic photocatalyst. Colloids Surfaces A. 2006; 289(1-3): 47-52.
2. Daneshvar N, Aber S, Khani A, et al. Study of imidaclopride removal from aqueous solution by adsorption onto granular activated carbon using an on-line spectrophotometric analysis system. J Hazard Mater. 2007; 144(1-2): 47-51.
3. Daneshvar N, Aber S, Khani A, et al. Investigation of adsorption kinetics and isotherms of imidacloprid as a pollutant from aqueous solution by adsorption onto industrial granular activated carbon. J Food Agri Environ. 2007; 5(3-4): 425-9.
4. Walker S, Narbaitz RM. Hollow fiber ultrafiltration of Ottawa river water: Floatation versus sedimentation pre-treatment. Chem Eng J. 2016; 288: 228-37.
5. Okolo BI, Naji PC, Onukwuli OD. Nephelometric approach to study coagulation-flocculation of brewery effluent medium using detarium

[Downloaded from jehsd.ssu.ac.ir on 2025-09-12]
[DOR: 20.1001.1.24766267.2019.4.1.5.3]
[DOI: 10.18502/jehsd.v4i1.486]

Microcarpum seed powder by response surface methodology. J Environ Chem Eng. 2016; 4(1): 992-1001.
6. Gupta M K, Mitta AK. Integrated biological and advanced oxidation based treatment of Hexamine bearing wastewater: Effect of cow-dung as a co-substrate. J Hazard Mater. 2016; 308: 394-401.
7. Khani A, Sohrabi MR, Khosravi M, et al. Enhancing purification of an azo dye solution in nanosized zero-valent iron-ZnO photocatalyst system using subsequent semi batch packed-bed reactor. Turkish J Eng & Environ Sci. 2013; 37(1): 91-9.
8. Khani A, Pezeshki B. Easy simultaneous synthesis–immobilization of nanosized CuO-ZnO on perlite as a photocatalyst for degradation of acid orange 7 from aqueous solution in the presence of visible light. Desalination Water Treat. 2015; 57: 7047-53.
9. Khani A, Sohrabi MR. Simultaneous synthesis-immobilization of nano ZnO on perlite for photocatalytic degradation of an azo dye in semi batch packed bed photoreactor. Polish J Chem Tech. 2012; 14(4): 69-76.
10. Kanel SR, Manning B, Charlet L, et al. Removal of Arsenic(III) from groundwater by Nanoscale Zero-valent Iron. Environ Sci Technol. 2005; 39(5): 1291-8.
11. Schrick B, Blough JL, Jones AD, et al. Hydrodechlorination of trichloroethylene to hydrocarbons using bimetallic nickel-iron nanoparticles. Chem Mater. 2002; 14: 5140-7.
12. Zhang WXJ. Nanoscale iron particles for environmental remediation: an overview. J Nanopart Res. 2003; 5: 323-32.
13. Khani A, Sohrabi MR, Khosravi M, et al. Decolorization of an azo dye from aqueous solution by nano zero-valent iron immobilized on perlite in semi batch packed bed reactor. Fresenius Environ Bull. 2012; 21: 2153-9.
14. Chang JH, Cheng SF. The remediation performance of a specific electrokinetics integrated with zero-valent metals for perchloroethylene contaminated soils. J Hazard Mater. 2006, 131(1-3): 153-62.
15. Xiong Z, Zhao DY, Pan G. Rapid and complete destruction of perchlorate in water and ion-exchange brine using stabilized zero-valent iron nanoparticles. Water Res. 2007; 41(15): 3497-505.
16. Ponder SM, Darab JG, Mallouk TE. Remediation of Cr(VI) and Pb(II) aqueous solutions using supported nanoscale zero-valent iron. Environ Sci Technol. 2000; 34: 2564-9.
17. Hu J, Lo IMC, Chen GH. Fast removal and recovery of Cr (VI) using surface modified Jacob site ($MnFe_2O_4$) nanoparticles. Langmuir. 2005; 39(18): 11173-9.
18. Bayramoglu M, Kobya MOT, Sozbir M. Operating cost analysis of electrocoagulation of textile dye wastewater. Sep Purif Technol. 2004; 37(2): 117-25.
19. Chang MC, Shu HY, Yu HH. An Integrated technique using zero-valent iron and UV/H_2O_2 sequential process for complete decolorization and mineralization of CI Acid Black 24 wastewater. J Hazard Mater. 2006; 138(3): 574-81.
20. Shu HY, Chang MC, Chang C. Integration of nanosized zero-valent iron particles addition with UV/H_2O_2 process for purification of azo dye acid black 24 solutions. J Hazard Mater. 2009; 167(1-3): 1178-84.

[Downloaded from jehsd.ssu.ac.ir on 2025-09-12]
[DOR: 20.1001.1.24766267.2019.4.1.5.3]
[DOI: 10.18502/jehsd.v4i1.486]